FEBS Letters 499 (2001) 268–273 FEBS 24933

Amyloid-like fibrils from an 18-residue peptide analogue of a part of the central domain of the B-family of silkmoth chorion proteins

Vassiliki A. Iconomidou[a], Georgios D. Chryssikos[b], Vassilis Gionis[b], Gert Vriend[c], Andreas Hoenger[d], Stavros J. Hamodrakas[a,*]

[a] *Department of Cell Biology and Biophysics, Faculty of Biology, University of Athens, Panepistimiopolis, Athens 157 01, Greece*
[b] *Theoretical and Physical Chemistry Institute, National Hellenic Research Foundation, Athens 116 35, Greece*
[c] *CMBI, KUN, Toernooiveld 1, 6525 ED Nijmegen, The Netherlands*
[d] *European Molecular Biology Laboratory, Meyerhofstrasse 1, Postfach 10.2209, D-69117 Heidelberg, Germany*

Received 5 February 2001; accepted 7 May 2001

First published online 8 June 2001

Edited by Gunnar von Heijne

Abstract Chorion is the major component of silkmoth eggshell. More than 95% of its dry mass consists of the A and B families of low molecular weight structural proteins, which have remarkable mechanical and chemical properties, and protect the oocyte and the developing embryo from the environment. We present data from negative staining, Congo red binding, X-ray diffraction, Fourier transform-Raman, attenuated total reflectance infrared spectroscopy and modelling studies of a synthetic peptide analogue of a part of the central domain of the B family of silkmoth chorion proteins, indicating that this peptide folds and self-assembles, forming amyloid-like fibrils. These results support further our proposal, based on experimental data from a synthetic peptide analogue of the central domain of the A family of chorion proteins, that silkmoth chorion is a natural, protective amyloid [Iconomidou et al., FEBS Lett. 479 (2000) 141–145].

Key words: Silkmoth chorion protein; Amyloid fibril; Electron microscopy; X-ray diffraction; Fourier transform-Raman spectroscopy; Attenuated total reflectance infrared spectroscopy; Modelling

1. Introduction

Amyloid fibril formation is a specific and ordered aggregation process [2], which is associated with a group of serious diseases including Alzheimer's, the transmissible spongiform encephalopathies, type II diabetes mellitus and a number of systemic polyneuropathies [3–6]. These neurodegenerative diseases have attracted the interest of numerous laboratories, which are trying to reveal the mechanisms of peptide and protein self-assembly to form insoluble non-covalent β-sheet-rich quaternary structures. For this research, the most common sources are proteins denatured in vitro and synthetic peptides of low molecular weight, which often form fibrils spontaneously. Apart from the cross-β structure with the β-strands perpendicular to the fiber axis [7,8] these fibrils share two common characteristics: they bind Congo red [9] and they are seen as uniform (ca. 100 Å) unbranched fibrils of indefinite length [10], which may be straight or slightly curved [11,12].

Chorion is an important biological structure with extraordinary mechanical and physiological properties, and it constitutes the major part (ca. 90%) of the eggshell of many insect and fish eggs [13]. The proteinaceous silkmoth chorion consists of more than 200 different proteins, which account for more than 95% of its dry mass [13]. Silkmoth chorion proteins are variants of two major themes, and have been classified into two major classes, A and B [14]. Both families of silkmoth chorion proteins consist of three domains [15]. The central domain is conserved in both classes. The flanking N- and C-terminal domains are more variable and contain characteristic tandem repeats [15]. A and B central domains show distant similarities, suggesting that the chorion genes constitute a superfamily derived from a single ancestral gene [16].

To study chorion protein structural properties, we synthesized peptide analogue representatives of parts or the whole of the central conservative domain of the two silkmoth chorion protein families, A and B [17]. This was because it proved very difficult to purify individual chorion proteins in large enough amounts of sufficient purity for structural studies. The central domains of the A and B families of chorion proteins are highly conserved in both sequence and length and probably this conservation indicates that these domains play an important functional role in the formation of silkmoth chorion structure [18].

We have recently shown that a 51-residue peptide analogue of the central domain of the A family of silkmoth chorion proteins (cA peptide) forms amyloid-like fibrils in vitro by self-assembly, under a great variety of conditions [1]. This probably suggests that silkmoth chorion is a natural amyloid with protective properties important for the survival and development of the oocyte and the developing embryo [1]. The cA peptide exhibits characteristic six-residue periodicities and it is a convenient model system to study amyloid fibril formation and assembly [1].

In this work, we present the amyloid characteristics of another 18-residue peptide (B peptide) representative of part of the central conservative domain of the B family silkmoth chorion proteins (Fig. 1). The data presented in this study support our choice of chorion protein peptide analogues as model systems to study mechanisms of amyloid-like fibril formation

*Corresponding author. Fax: (30)-1-7274742.
E-mail: shamodr@cc.uoa.gr
E-mail: veconom@cc.uoa.gr
E-mail: gdchryss@eie.gr
E-mail: vriend@cmbi.kun.nl
E-mail: hoenger@embl-heidelberg.de

0014-5793/01/$20.00
PII: S0014-5793(01)02510-8

and assembly, and provide clues for chorion structure formation.

2. Materials and methods

2.1. Formation of amyloid-like fibrils

B peptide (Fig. 1), synthesized as described in [17], was dissolved in distilled water (pH 5.5) at a concentration of 10 mg ml^{-1}. It was found to produce gels spontaneously after 1 month incubation. These gels contain fibrils, which have tinctorial, morphological and structural characteristics resembling those of amyloid fibrils (see below).

2.2. Negative staining

For negative staining, B peptide fibril suspensions were applied to glow-discharged 400-mesh carbon-coated copper grids for 60 s. The grids were flash-washed with ca. 150 μl of distilled water and stained with a drop of 1% (w/v) aqueous uranyl acetate for 45 s. Excess stain was removed by blotting with a filter paper and the grids were air-dried. They were examined in a Philips CM120 Biotwin transmission electron microscope operated at 100 kV. Photographs were obtained with a Gatan 694 retractable slow-scan CCD camera, with a Peltier-cooled chip, mounted at the bottom flange (Gatan Inc.), utilizing the program Digital Micrograph 2.5.8 (Gatan Inc.).

2.3. Congo red staining and polarized light microscopy

B peptide fibril suspensions were applied to glass slides and stained with a 10 mM Congo red (Sigma) solution in phosphate-buffered saline (pH 7.4) for approximately 2 h. They were then washed several times with 90% ethanol and left to dry. Subsequently, the samples were observed under bright field illumination and between crossed polars, using a Zeiss KL 1500 polarizing stereomicroscope equipped with an MC 80 DX camera.

2.4. X-ray diffraction

A 10-μl droplet of fibril suspension was placed between two siliconized glass rods, spaced ca. 2 mm apart and mounted horizontally, as collinearly as possible. It was allowed to equilibrate at ambient temperature and humidity for 30 min to form a fiber suitable for X-ray diffraction. X-ray diffraction patterns were obtained immediately from these fibers and were recorded on a Mar Research 345-mm image plate, utilizing double-mirror (Prophysics mirror system XRM-216), focused CuK_α radiation ($\lambda = 1.5418$ Å), obtained from a GX-21 rotating anode generator (Elliot-Marconi Avionics, Hertfordshire, UK) operated at 40 kV, 75 mA. The specimen-to-film distance was set at 150 mm and the exposure time was 30 min. No additional low angle reflections were observed at longer specimen-to-film distances. The X-ray patterns, initially viewed using the program MarView (Mar Research, Hamburg, Germany), were displayed and measured with the aid of the program IPDISP of the CCP4 package [19].

2.5. Fourier transform (FT)-Raman spectroscopy

For the Raman measurements, the oriented fiber of the B peptide, mounted on a siliconized glass rod and previously used as a sample for X-ray diffraction measurements, was employed. Raman spectra were obtained on a Fourier transform instrument (Bruker RFS 100) employing for excitation ca. 400 mW of the Nd:YAG 1064 nm line in a backscattering geometry. Excitation in the near infrared greatly reduces the fluorescence of the sample and eliminates the need for prolonged laser annealing, which is necessary if excitation in the visible range is employed instead. The resolution was 4 cm^{-1} and the total acquisition time was 10 h (ca. 10 000 scans). The interferograms were Fourier-transformed in 1-h acquisition time segments to allow the detection of time-dependent phenomena (sample degradation, luminescence, bleaching, etc). Subsequently, the spectra were averaged and the standard deviation (σ) was calculated.

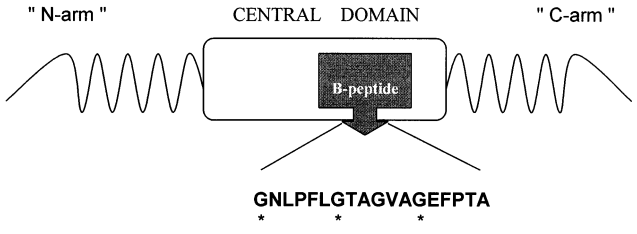

Fig. 1. A schematic representation of the tripartite structure of silkmoth chorion proteins of the B family. A highly conservative central domain of invariant length and two more variable flanking 'arms' constitute each protein. Characteristic, tandemly repeating peptides are present both in the central domain and in the 'arms' ([18] and references therein). The amino acid sequence and relative position of the synthetic B peptide (one-letter code), designed to be an analogue of a part of the central domain of the B family, is shown. Invariant glycines repeating every six residues are marked with an asterisk below the sequence.

2.6. Attenuated total reflectance infrared spectroscopy (ATR FT-IR)

Infrared spectra were obtained at a resolution of 2 cm^{-1} on a Fourier transform instrument (Bruker Vector 22) equipped with a single reflection Ge attenuated total reflectance accessory (Thunderdome by Spectra Tech). Internal reflection spectroscopy has several advantages compared to the more common KBr dispersion technique [20]. The choice of ATR was dictated by the need to exclude any possible spectroscopic and chemical interactions between the sample and the dispersing medium. Having a penetration depth of less than 1 μm (1000 cm^{-1}, Ge), ATR is free of saturation effects, which may be present in the transmission spectra of thicker samples. Moreover, the use of a single reflection accessory facilitates the acquisition of data from small samples. In the present investigation, B peptide fibril suspensions in distilled water were allowed to form thin films deposited directly on the surface of the Ge element by evaporating the solvent under a dry N_2 flow. Five 400-scan spectra were collected and averaged to improve the signal-to-noise ratio. The spectra were corrected for the effect of wavelength on the penetration depth (p.d. $\propto \lambda$). The corresponding effect of the (frequency-dependent) refractive index (n) of the samples was not taken into account due to the lack of relevant data.

2.7. Post-run computations of the spectra

The Raman scattering and infrared ATR absorption peak maxima were determined from the minima in the second derivative of the corresponding spectra. Derivatives were computed analytically using routines of the Bruker OPUS/OS2 software and included smoothing by the Savitzky–Golay algorithm over a ± 4 cm^{-1} (infrared), or ± 8 cm^{-1} (Raman) range, around each data point [21]. Smoothing over narrower ranges resulted in a deterioration of the signal-to-noise ratio and did not increase the number of minima that could be determined with confidence.

2.8. Modelling

Modelling was performed following the same procedures described by Iconomidou et al. [1].

3. Results and discussion

Twisted and non-twisted ribbons are constituents of the gels formed by self-assembly after dissolving the B peptide in distilled water, pH 5.5 (see Section 2 and Fig. 2). Each twisted ribbon consists of thin protofilaments (fibrils) that have a tendency to coalesce laterally among each other (Fig. 2). The protofilaments have a uniform diameter of approximately 30–40 Å. They associate sideways to form twisted and non-twisted ribbons of variable width. Similar twisted ribbons have been observed in amyloid fibrils formed by fusion peptides [22], an SH3 domain [23], various Alzheimer's disease peptides [24] and a peptide from the adenovirus fiber shaft [12], to mention just a few examples. 'Beading' is evident along the protofilaments (fibrils), indicating that they probably have a helical structure [25]. The 'beads' have dimensions of the order of ca. 30 Å. Congo red-stained B peptide gels (see Section 2) showed the red-green (yellow) birefringence characteristic of amyloid fibrils when viewed under crossed polars (Fig. 3).

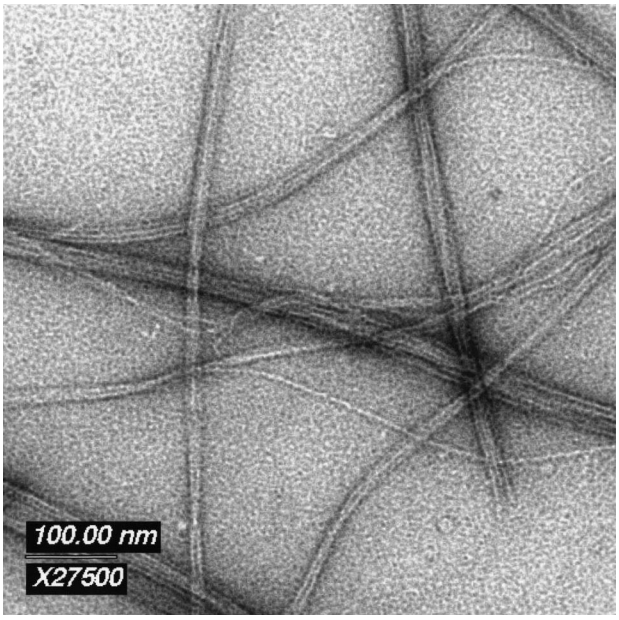

Fig. 2. Electron micrograph of amyloid-like fibrils derived by self-assembly from a 10 mg/ml solution of the B peptide in distilled water, pH 5.5. Fibrils are negatively stained with 1% uranyl acetate. The protofilaments (fibrils) are 30–40 Å in diameter and they self-assemble laterally into twisted and non-twisted ribbons of indeterminate thickness and length (several micrometers) forming gels (not shown). Individual protofilaments have a 'beaded' appearance, suggesting a helical structure. The 'beads' have a diameter of ca. 25–30 Å.

Suspensions of the fibril-containing gels seen in Fig. 2 form fibers (see Section 2). X-ray diffraction patterns (Fig. 4) taken from these fibers showed four major reflections at 4.64, 5.20, 9.14 and 26.00 Å. These reflections appear as rings due to the poor alignment of the constituent fibrils. Several attempts were made to obtain oriented specimens, but they were not successful. This is probably due to random packing of the ribbons in the gels, which adopt all possible orientations (see Fig. 2) as confirmed by electron microscopy (data not shown).

The strong and relatively sharp reflection corresponding to a periodicity of 4.64 Å and the weaker one at 9.14 Å may be attributed to β-sheet structure present in the fibrils (inter-strand and inter-sheet distances respectively). These reflections are characteristic of the 'cross-β' conformation [26] observed for several amyloid-like fibrils ([1,2] and references therein), in which the β-strands are oriented perpendicular to the fibril axis and the sheets run mainly parallel to the fibril axis. This conformation would produce oriented patterns from oriented samples with the ca. 4.7 Å reflection meridional and the ca. 10 Å reflection equatorial, as in the oriented patterns obtained from fibers of the chorion cA peptide [1]. In the case of the B peptide fibrils, efforts to obtain oriented samples were not successful as described above, and thus the diffraction patterns contained diffraction rings instead of oriented reflections. A similar case to ours, where non-oriented X-ray diffraction patterns were observed, is clearly that of a peptide from the adenovirus fiber shaft [12], which also produces amyloid-like fibrils. The reflection at 26 Å may arise from the lateral packing of the fibrils when forming the ribbons or, perhaps, it is due to the repeating 'beaded' structure along the protofilaments (Fig. 2). The origin of the 5.2 Å reflection is not clear. It might simply be the fifth order of the 26 Å reflection. However, no additional data are available to explain its presence.

Spectral acquisition by ATR FT-IR and FT-Raman spectroscopy has been shown to yield rich information about the secondary structure of the B peptide, without the drawbacks

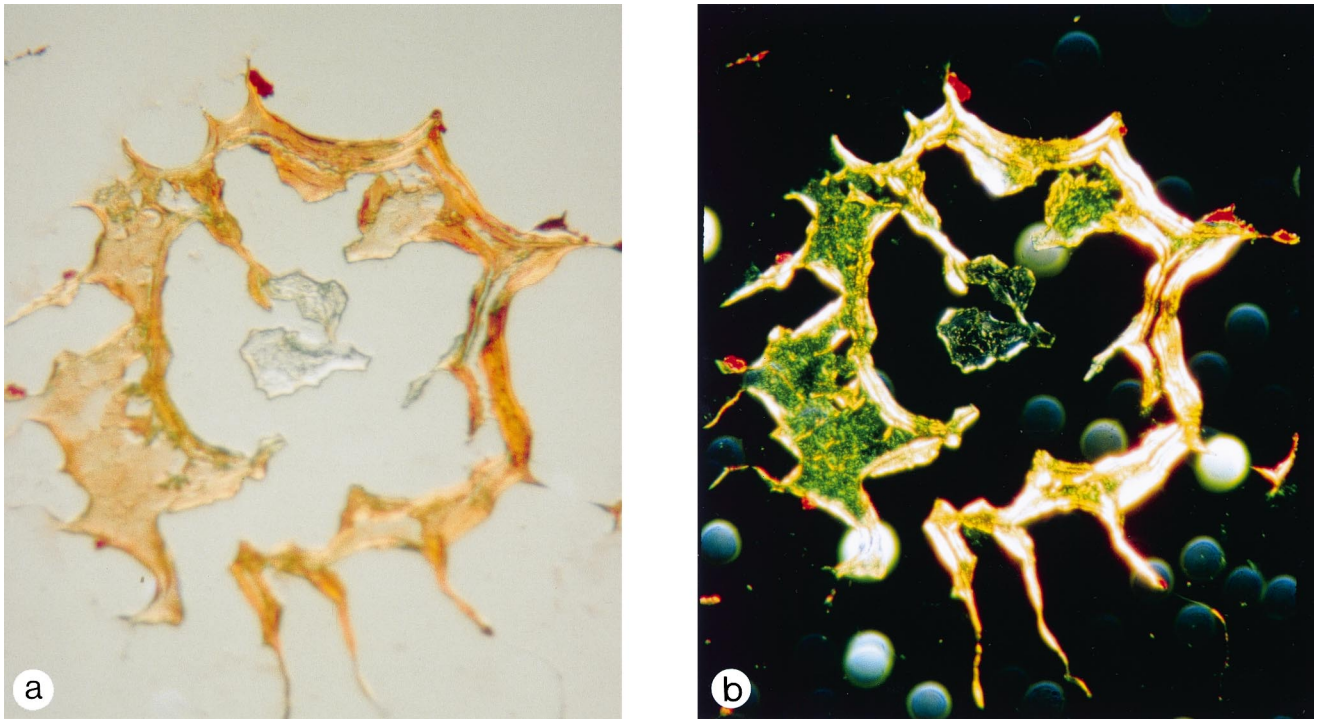

Fig. 3. Photomicrographs of B peptide fibrils stained with Congo red. a: Bright field illumination. b: Crossed polars. The red-green birefringence characteristic of amyloid fibrils is clearly seen.

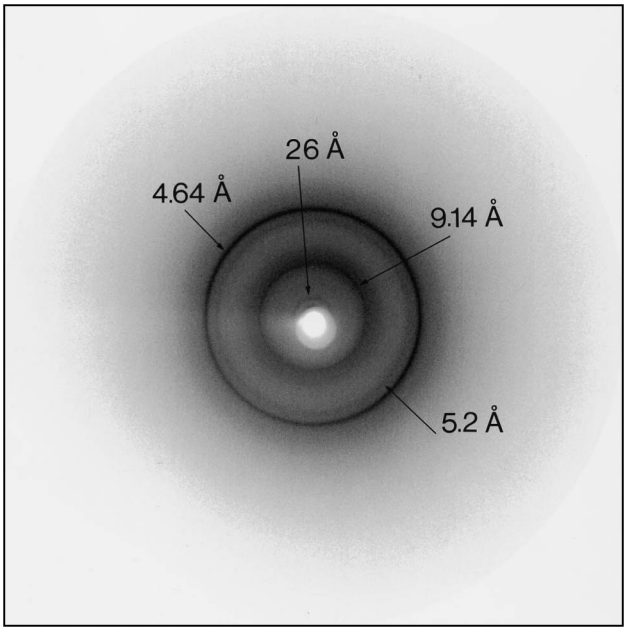

Fig. 4. X-ray diffraction pattern from a fiber of B peptide amyloid-like fibrils (see Section 2). Four reflections, which correspond to structural repeats of 4.64, 5.20, 9.14 and 26 Å, are marked by arrows. The two most prominent at 4.64 and 9.14 Å, which probably correspond to the spacing of adjacent β-strands and to the packing distance of β-sheets respectively, indicate the presence of β-sheets ('cross-β' sheets) in the structure of the fibrils. Due to the poor alignment of fibrils these reflections appear as rings. The reflection at 26 Å is either due to the packing of the fibrils or originates from the 'beaded' sub-structure along the fibrils (see Fig. 2). The origin of the 5.2 (= 1/5 of 26) Å reflection is not known.

associated with the more conventional vibrational techniques [27]. A detailed analysis of the vibrational trends associated with the organization of peptide analogues of silkmoth chorion proteins into amyloid fibrils is in preparation (Paipetis, Iconomidou, Gionis, Chryssikos and Hamodrakas, in preparation). Within the scope of this paper, Table 1 shows the most prominent bands and their tentative assignments in the FT-Raman spectrum of the B peptide, utilizing as sample the fiber used for the X-ray diffraction experiment (Fig. 5).

In the amide I region of the Raman spectrum, the band at 1669 cm^{-1} (Fig. 5) suggests the presence of β-sheet conformation in the structure of the B peptide, when it forms amyloid-like fibrils in the fiber used for X-ray diffraction experiments ([28] and references therein). Analysis of the amide I band of the FT-Raman spectrum (Fig. 5) using the method of Hamodrakas et al. [29] suggests that there is 64% antiparallel β-sheet and 30% β-turns in the B peptide structure. The presence of a strong band at 1229 cm^{-1} in the conformationally sensitive amide III region (Fig. 5), a characteristic signature of β-pleated sheet ([28] and references therein), strongly supports the amide I evidence as well as the X-ray diffraction data. Bands at ca. 620, 1003, 1033 and 1603 cm^{-1} are most likely due to the two Phe residues present in the B peptide (Fig. 1).

Table 1
Main FT-Raman bands (600–1800 cm^{-1}) and tentative assignments in the FT-Raman spectrum of B peptide

Band	Assignment
620	Phe
832	ν(C–C)
859	ν(C–C) of Pro ring
886	skeletal stretch
925	ν(C–C) of Pro ring
1003	Phe
1033	Phe
1087	ν(C–N)
1229	**Amide III (β-sheet)**
1318	ν(C–N)
1341	δ(CH)
1403	$\nu_s(COO^-)$
1453	$\delta(CH_2, CH_3)$
1605	Phe
1669	**Amide I (β-sheet)**

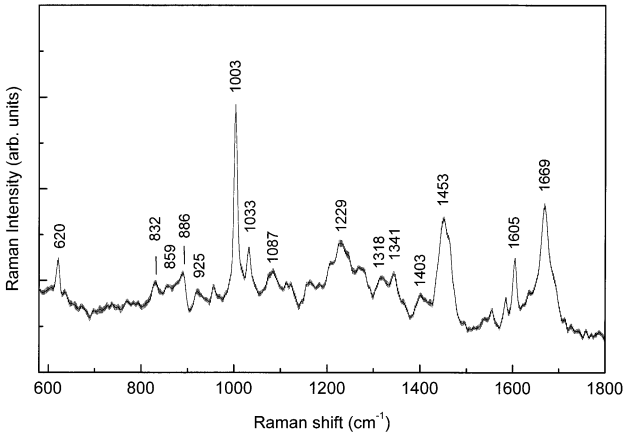

Fig. 5. FT-Raman spectrum of B peptide amyloid-like fibrils in the range 600–1800 cm^{-1}. Error bars equal the standard deviation (σ) of the measurement. The spectrum has been acquired from the fiber used to obtain the X-ray diffraction pattern of Fig. 4.

Concomitant evidence for the preponderance of β-sheet in amyloid-like fibrils derived from the B peptide is given by ATR FT-IR spectroscopy (Fig. 6). The ATR FT-IR spectrum shows one prominent band at 1623 cm^{-1} in the amide I region. This band is clearly due to β-sheet conformation [29]. Its relatively low wavenumber may be attributed to strong hydrogen bonds in the β-sheets [29], whereas the fact that it is sharp (its half-width is ca. 20 cm^{-1}) suggests that the distribution of the ϕ and ψ angles in the sheets is rather narrow, which means a very uniform structure. This is also true for the amide I band of the FT-Raman spectrum (Fig. 5). Its apparent half-width is ca. 17 cm^{-1}, lower than that of the very uniform silk

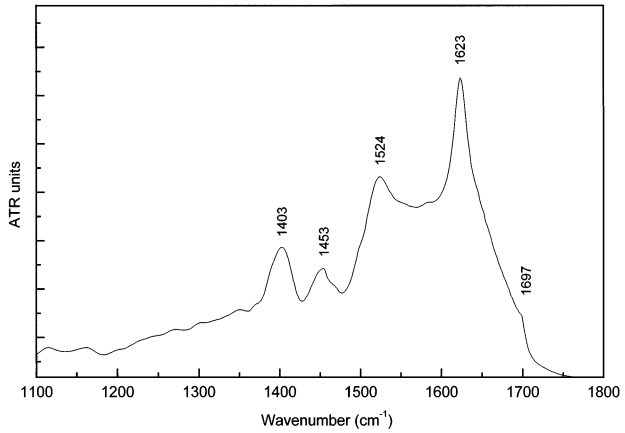

Fig. 6. ATR FT-IR spectrum of B peptide amyloid-like fibrils (see Section 2) in the range 1100–1800 cm^{-1}.

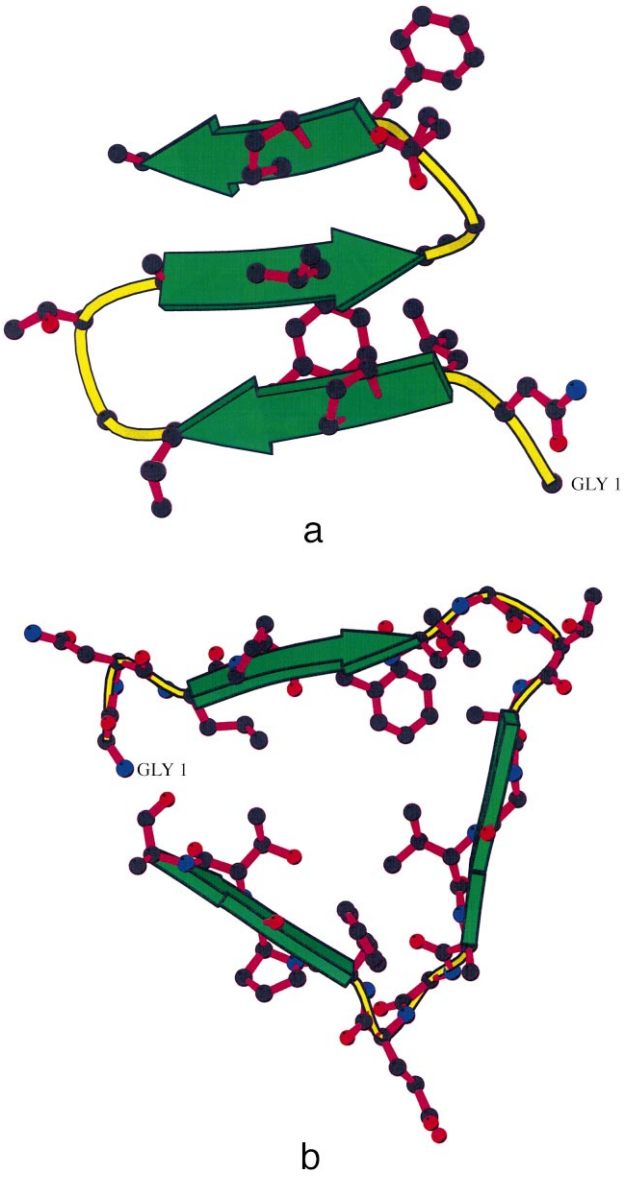

Fig. 7. a: Antiparallel twisted β-sheet model ('cross-β' structure) proposed for the B peptide (ribbon representation [33], with side chains added as balls and sticks). Arrows represent β-strands. Tentative type II′ β-turns alternate with four-residue β-strands [1,18,31,32]. View perpendicular to a 'face' of the sheet. b: A ribbon representation of the B peptide in a left-handed parallel β-helix conformation (ca. one turn of the helix) with side chains added as balls and sticks. Tentative type II β-turns alternate with β-strands. Arrows represent β-strands. View parallel to the axis of the helix.

fibroin (ca. 27 cm^{-1}) ([28] and references therein). The infrared shoulder at 1697 cm^{-1} is a strong indication that the β-sheets are antiparallel [27,29,30], in good agreement with the analysis of the amide I band of the FT-Raman spectrum. Thus, both FT-Raman and ATR FT-IR support the presence of uniform antiparallel β-sheets in the structure of B peptide fibrils, apparently in agreement with the existence of a 'cross-β' structure implied by X-ray diffraction and Congo red binding data.

Taking into account all experimental and theoretical evidence accumulated previously for silkmoth chorion proteins [18,31,32], as well as for synthetic peptide analogues of parts of chorion proteins [1], the hexapeptide periodicities present in the central domain of the B family of chorion proteins, and the fact that the central domain of B proteins is distantly homologous to the A proteins ([18] and references therein), we produced as structural models for the B peptide, the models presented in Fig. 7a,b by homology modelling. The procedure followed closely that described in [1]. The data presented here are clearly in favor of the antiparallel β-pleated sheet model shown in Fig. 7a, but it should be mentioned that the left-handed parallel β-helix model of Fig. 7b has attractive features as well. Most interesting among these is the hydrophobic core and hydrophobic faces of the triangular prism-like helix. Nevertheless, the 'edges' of this prism are occupied by charged, polar residues and glycines and this makes three-dimensional packing difficult, unless there are very specific interactions. The hydrophobic faces of the antiparallel β-sheet structure shown in Fig. 7a facilitate uniform three-dimensional packing of the β-sheets, leaving the polar and charged residues on both lateral 'edges' of the sheet for favorable lateral interactions. This is actually observed in the ribbons of Fig. 2, which are formed by sideways association of protofilaments. It can easily be envisaged that layers of such ribbons might be the basic constituents of silkmoth chorion structure, primarily a lamellar structure ([18] and references therein), formed from layers of fibrils [25]. Thus, our previous proposal that silkmoth chorion is a natural protective amyloid is further supported by the results of this study. Further work is in progress to test these ideas by careful design of suitable peptide mutants.

Acknowledgements: We thank Dr. L. Serrano, Dr. M. Saraste, Mr. P. Everitt and Mr. K. Goldie for their help with the experiments. We thank Dr. A. Paipetis for his assistance with FT-Raman data acquisition. Special thanks are due to Prof. F.C. Kafatos for his unfailing interest and help. Financial support of this work was provided by the Greek General Secretariat of Research and Technology (Grant 99ED8), the University of Athens and the National Hellenic Research Foundation. V.A.I. and S.J.H. gratefully acknowledge the help of the EMBL summer visitors program.

References

[1] Iconomidou, V.A., Vriend, G. and Hamodrakas, S.J. (2000) FEBS Lett. 479, 141–145.
[2] Sunde, M. and Blake, C. (1997) Adv. Protein Chem. 50, 123–159.
[3] Pepys, M.B. (1996) in: The Oxford Textbook of Medicine, 3rd edn. (Weatherall, D.J., Ledingham, J.G.G. and Warell, D.A., Eds.), Vol. 2, pp. 1512–1524, Oxford University Press, Oxford.
[4] Kelly, J.F. (1996) Curr. Opin. Struct. Biol. 6, 11–17.
[5] Kelly, J.F. (1998) Curr. Opin. Struct. Biol. 8, 101–106.
[6] Dobson, C.M. (1999) Trends Biochem. Sci. 24, 329–332.
[7] Glenner, G.G. (1980) New Engl. J. Med. 302, 1283–1292.
[8] Glenner, G.G. (1980) New Engl. J. Med. 302, 1333–1343.
[9] Glenner, G.G., Eanes, E.D. and Page, D.L. (1972) J. Histochem. Cytochem. 20, 821–826.
[10] Cohen, A.S., Shirahama, T. and Skinner, M. (1981) Electron Microscopy of Protein, (Harris, I., Ed.), Vol. 3, pp. 165–205, Academic Press, London.
[11] Sunde, M. and Blake, C.C.F. (1998) Q. Rev. Biophys. 31, 1–39.
[12] Luckey, M., Hernandez, J.-F., Arlaud, G., Forsyth, V.T., Ruigrok, R.W.H. and Mitraki, A. (2000) FEBS Lett. 468, 23–27.
[13] Kafatos, F.C., Regier, J.C., Mazur, G.D., Nadel, M.R., Blau, H.M., Petri, W.H., Wyman, A.R., Gelinas, R.E., Moore, P.B., Paul, M., Efstratiadis, A., Vournakis, J.N., Goldsmith, M.R., Hunsley, J.R., Baker, B., Nardi, J. and Koehler, M. (1982) in: Results and Problems in Cell Differentiation (Beerman, W., Ed.), Vol. 8, pp. 45–145, Springer-Verlag, Berlin.

[14] Regier, J.C. and Kafatos, F.C. (1985) in: Comprehensive Insect Biochemistry, Physiology and Pharmacology (Gilbert, L.I. and Kerkut, G.A., Eds.), Vol. 1, pp. 113–151, Pergamon Press, Oxford.
[15] Hamodrakas, S.J., Jones, C.W. and Kafatos, F.C. (1982) Biochim. Biophys. Acta 700, 42–51.
[16] Lekanidou, R., Rodakis, G.C., Eickbush, T.H. and Kafatos, F.C. (1986) Proc. Natl. Acad. Sci. USA 83, 6514–6518.
[17] Benaki, D.C., Aggeli, A., Chryssikos, G.D., Yiannopoulos, Y.D., Kamitsos, E.I., Brumley, E., Case, S.T., Boden, N. and Hamodrakas, S.J. (1998) Int. J. Biol. Macromol. 23, 49–59.
[18] Hamodrakas, S.J. (1992) in: Results and Problems in Cell Differentiation (Case, S.T., Ed.), Vol. 19, pp. 115–186, Springer-Verlag, Berlin.
[19] Collaborative Computational Project (1994) Number 4 The CCP4 Suite: Programs for Protein Crystallography, Acta Crystallogr. D50, 760–763.
[20] de Jongh, H.H.J., Goormaghtigh, E. and Ruysschaert, J.M. (1996) Anal. Chem. 242, 95–103.
[21] Savitsky, A. and Golay, M.J.E. (1964) Anal. Chem. 36, 1627–1639.
[22] Ulrich, A.S., Tichelaar, W., Forster, G., Zschornig, O., Weinkauf, S. and Meyer, H.W. (1999) Biophys. J. 77, 829–841.
[23] Jimenez, J.L., Guijarro, J.I., Orlova, E., Zurdo, J., Dobson, C.M., Sunde, M. and Saibil, H.R. (1999) EMBO J. 18, 815–821.
[24] Fraser, P.E., Nguyen, J.T., Surewicz, W.K. and Kirschner, D.A. (1991) Biophys. J. 60, 1190–1201.
[25] Hamodrakas, S.J., Margaritis, L.H., Papassideri, I. and Fowler, A. (1986) Int. J. Biol. Macromol. 8, 237–242.
[26] Geddes, A.J., Parker, K.D., Atkins, E.D.T. and Beighton, E. (1968) J. Mol. Biol. 32, 343–358.
[27] Iconomidou, V.I., Chryssikos, G.D., Gionis, V., Pavlidis, M.A., Paipetis, A. and Hamodrakas, S.J. (2001) J. Struct. Biol. (in press).
[28] Hamodrakas, S.J., Asher, S.A., Mazur, G.D., Regier, J.C. and Kafatos, F.C. (1982) Biochim. Biophys. Acta 703, 216–222.
[29] Surewicz, W.K., Mantsch, H.H. and Chapman, D. (1993) Biochemistry 32, 389–394.
[30] Krejchi, M., Cooper, S.J., Deguchi, Y., Atkins, E.D.T., Fournier, M.J., Mason, T.L. and Tirrell, D.A. (1997) Macromolecules 30, 5012–5024.
[31] Hamodrakas, S.J., Etmektzoglou, T. and Kafatos, F.C. (1985) J. Mol. Biol. 186, 583–589.
[32] Hamodrakas, S.J., Bosshard, H.E. and Carlson, C.N. (1988) Protein Eng. 2, 201–207.
[33] Kraulis, P.J. (1991) J. Appl. Crystallogr. 24, 946–950.